Processing and Application of Ceramics 13 [3] (2019) 257–268
https://doi.org/10.2298/PAC1903257B

Influence of molar ratio on dielectric, ferroelectric and magnetic properties of $Co_{0.5}Mg_{0.5}Fe_2O_4/Ba_{0.85}Sr_{0.15}TiO_3$ composite ceramics

Lang Bai[1], Rongli Gao[2,3,*], Qingmei Zhang[4,5], Zhiyi Xu[6], Zhenhua Wang[2,3], Chunlin Fu[2,3], Gang Chen[2,3], Xiaoling Deng[2,3], Wei Cai[2,3,*]

[1]*School of Materials and Engineering, Panzhihua University, Panzhihua 617000, China*
[2]*School of Metallurgy and Materials Engineering, Chongqing University of Science and Technology, Chongqing 401331, China*
[3]*Chongqing Key Laboratory of Nano/Micro Composite Materials and Devices, Chongqing 401331, China*
[4]*National Laboratory of Solid State Microstructures, Nanjing University, Nanjing 210093, China*
[5]*School of Applied Science, Taiyuan University of Science and Technology, Taiyuan 030024, China*
[6]*National Institute of Metrology, Beijing 100029, China*

Received 7 January 2019; Received in revised form 22 May 2019; Accepted 4 August 2019

Abstract

In the present work, $Co_{0.5}Mg_{0.5}Fe_2O_4/Ba_{0.85}Sr_{0.15}TiO_3$ (CMFO/BST) composite ceramics with different molar ratios (1:1, 1:2, 1:4, 1:6 and 1:8) were prepared by sol-gel method and sintered at 1150 °C. The effects of molar ratio on the structure, dielectric and multiferroic properties were comparatively studied. The results indicate that all the synthesized composites mainly show bi-phase structure except slight presence of impurity phases. The surface of the specimens is relatively dense and the mean grain size is about 2 μm. It decreases at first and then increases with the increased molar ratio. The dielectric constant shows decreased trend with increasing the molar ratio, while the dielectric loss presents the opposite behaviour. With the increase of molar ratio, the height of the relaxation peak decreases while the peak position shifts to higher temperature range. The relaxation peak evolves gradually from one to two peaks. The residual polarization increases with voltage but decreases with frequency. The maximal polarization of 1.28 μC/cm² is obtained in the specimen with the molar ratio of 1:8, due to the largest concentration of ferroelectric phase BST. The magnetization shows abnormal behaviour with the change in molar ratio. The largest saturation and remnant magnetization are 20.89 and 12.66 emu/g, respectively when the molar ratio is 1:2 due to the stronger interface interaction effect between the two phases.

Keywords: *multiferroics, composite, dielectric properties, ferroelectric, magnetic*

I. Introduction

Multiferroic material is a new kind of functional material which can show magnetic and ferroelectric properties simultaneously [1–3]. In the past several decades, multiferroic materials have attracted great attention not only due to their intriguing physical properties, but also because of their potential applications in sensor, capacitor, information storage, energy harvesting, spintronics etc. [4–6]. Especially, the magnetic properties in these materials can be regulated by external electric field and the ferroelectric properties can be tuned by magnetic as well. This phenomenon is usually called magnetoelectric (ME) effect. Significantly, multiferroics could lead to a new generation of memory devices that can be electrically written and magnetically read [7]. Strong ME effect at room temperature of multiferroic materials is the precondition of making these applications come true. However, this is limited in the single phase multiferroic materials, since the Curie temperature of the magnetic and (or) ferroelectric order is always far below room temperature. Due to $BiFO_3$ having high both the Curie temperature (~1100 K) and Neel temperature (~640 K) [8–10], a very few room temperature single

*Corresponding author: tel: +86 23 65023707,
e-mail: *gaorongli2008@163.com* (R. Gao)
caiwei_cqu@163.com (W. Cai)

phase multiferroic materials are known so far. The ME effect is still very weak because of the G-type antiferromagnetic ordering in bismuth ferrite and the serious leakage current induced by impurities and defects such as oxygen vacancies [11–13]. As a consequence, it is an important challenge to improve the ME effect from the practical application point of view.

Fortunately, this challenge may be overcome in biphase magnetoelectric composite, which is generally composed of room temperature magnetic material and ferroelectric material. In composite multiferroic materials, the magnetic and ferroelectric phases can respectively play their individual role and thus the limitation of the Curie temperature in single phase materials is non-existent. A well accepted coupling mechanism of composite multiferroic material is the interface interaction between the two phases, i.e. the result of magnetostriction and piezoelectric effect [14–16]. It is easy to speculate from the coupling mechanism that the ME effect in composite multiferroics depends strongly on the respective performance of the magnetic and ferroelectric phase. Up to now, many magnetic phases have been combined with various kinds of ferroelectric phases. For example, Fe_3O_4, MFe_2O_4 (M = Mg, Ca, Mn, Co, Ni, Cu, Zn, etc.) and (La,Ca)MnO_3 are usually chosen as the magnetic phase while $BiFeO_3$, (Ba,Sr)TiO_3, Ba(Zr,Ti)O_3 and Pb(Zr,Ti)O_3 have been used as the ferroelectric phase [17–21].

It should be pointed out that in addition to the intrinsic properties of the magnetic/ferroelectric phase, other factors, such as the molar ratio between the two phases, the grain size, the connective style as well as the dimensions have important effect on the ME behaviour [22–24]. Among them, molar ratio is one of the most important elements because it can determine the contact area between the two phases. In addition, proper molar ratio is able to balance the overall magnetic and ferroelectric performance and as a result excellent multiferroic properties may be obtained. Therefore, it is of great importance and significance to investigate how the molar ratio affects the multiferroic properties of magnetoelectric composites.

Herein, by using sol-gel method, we prepared $Co_{0.5}Mg_{0.5}Fe_2O_4/Ba_{0.85}Sr_{0.15}TiO_3$ (CMFO/BST) magnetoelectric composite ceramics and the effect of molar ratio (1:1, 1:2, 1:4, 1:6 and 1:8) on the dielectric, ferroelectric and magnetic properties have been investigated systematically. Therein, CMFO was chosen as the magnetic phase because of its preferable magnetization, chemical stability and better insulating properties, while BST presents superior ferroelectric properties and excellent dielectric properties especially the low dielectric loss.

II. Experimental procedure

2.1. Materials

All the raw materials used in this study were purchased from Sinopharm Chemical Regent Beijing Co. Ltd., including acetates ($Co(CH_3COO)_2 \cdot 4H_2O$, $Mg(CH_3COO)_2 \cdot 4H_2O$, $Fe(CH_3COO)_3$, $Ba(CH_3COO)_2$ and $Sr(CH_3COO)_2$), tetra-n-butyl titanate ($C_{16}H_{36}O_4Ti$), ethylene glycol ($(CH_2OH)_2$), ethanol (C_2H_6O), citric acid ($C_6H_8O_7$) and glacial acetic acid (CH_3COOH). All the reagents are used without further purification.

2.2. Synthesis of CMFO and BST particles

$(CH_2OH)_2$ and CH_3COOH were mixed with the volume ratio of 4 : 1. Then $Co(CH_3COO)_2$ was dissolved in the mixed solvent with constant stirring and then heated at 70 °C for 30 min to make sure that $Co(CH_3COO)_2$ could be dissolved completely, thus Co precursor solution was formed. Next, $Mg(CH_3COO)_2$ and $Fe(CH_3COO)_3$ were mixed with Co precursor solution. The pH of the mixed solution was adjusted to be ~4–5 by adding $HOCH_2CH_2NH_2$. Then $CH_3COCH_2COCH_3$ was added to control the hydrolysis rate. The concentration of the precursors in the solution was kept at ~0.3 mol/l by adjusting the amount of $C_4H_{10}O_2$. Finally, the solution was heated at 90 °C and continuously stirred, resulting in the xerogel of CMFO, followed by a heat treatment at 800 °C to burn out the organic solvent and form CMFO particles.

The BST particles can be prepared in a similar way. To prepare BST precursor solution, $Ba(CH_3COO)_2$, $Sr(CH_3COO)_2$ and $TiC_{12}H_{28}O_4$ were used as raw materials. Acetic acid and 2-ethoxyethanol were used as solvents. First, $Ba(CH_3COO)_2$ and $Sr(CH_3COO)_2$ were dissolved in 2-ethoxyethanol and acetic acid mixture (the volume ratio of 2-ethoxyethanol to acetic acid was 4 : 1) to form the Ba and Sr precursor solution. The mixture was stirred constantly, heated to 70 °C and maintained for 30 min to ensure that $Ba(CH_3COO)_2$ was dissolved completely. The Ti precursor solution was synthesized in a similar way. Next, Ba, Sr and Ti precursor solutions were mixed and stirred constantly for 30 min to form the BST precursor solution. The pH of the precursor solution was adjusted to 3 by adding ethanolamine (99.0% purity, Chengdu Kelong Chemical Reagent Factory). Then, acetylacetone was added to the solution to control the hydrolysis rate. The concentration of the precursor solution was subsequently adjusted to be 0.3 mol/l by adding a certain amount of 2-ethoxyethanol. Lastly, the mixture was heated at 90 °C. The obtained gel was heated at 400 °C to burn out the organic solvent, and then the calcined powders were ground for 8 h.

2.3. Fabrication of CMFO/BST composite ceramics

All particles weighted with various molar ratios (1:1, 1:2, 1:4, 1:6 and 1:8) were mixed with distilled water and then ball milled for 8 h. The obtained slurries were dried and then fired at 850 °C for 8 h, subsequently, the calcined powders were ground again for 8 h. The powder mixture was added into polyvinyl alcohol (PVA) solution. The concentration of PVA was 15% and the weight ratio between PVA and the composite particles

was 8 : 100. Finally, the treated composite powders were pressed at 15 MPa into 1 mm thick pellets with the diameter of 10 mm. The slices were sintered at 1150 °C for 4 h. Both sides of the sintered pellets were polished and a thin layer of silver was pasted on both sides and calcined at 500 °C for 30 min.

2.4. Characterization

The crystal structures of the prepared samples were analysed by X-ray diffraction (XRD, D/max 2500, Rigaku, Japan) using Cu-Kα radiation (λ = 1.5406 Å). Scanning electron microscope (FE-SEM, JSM-7800F, JEOL, Japan) was used to observe the morphology. The dielectric properties were determined by using a LCR instrument analyser (HP4980A, Agilent, USA) combined with a high temperature system (TZDM-RT-1000, China). The dielectric constant was calculated according to the following equation:

$$\varepsilon_r = \frac{C \cdot d}{\varepsilon_0 \cdot S} \tag{1}$$

where ε_r is the relative dielectric constant, C is the capacitance, d is the thickness, ε_0 is the vacuum dielectric constant (8.85×10^{-12} F/m), and S is the effective electrode area on the sample. The ferroelectric hysteresis loops were measured by ferroelectric test system (TF2000, aix-ACCT Inc., Germany). Magnetic hysteresis (M-H) loop measurements were carried out by using a vibrating sample magnetometer (VSM).

III. Results and discussion

3.1. Structural characterization

The X-ray diffraction patterns of the CMFO/BST composite ceramics are shown in Fig. 1. It is evident from the XRD patterns that all diffraction peaks of ferrite and ferroelectric phases emerge in the composite systems. The diffraction peaks 100, 110, 111, 200, 210, 211, 220 and 310 belong to the perovskite type tetragonal structure of BST with space group $P4mm$ (JCPDS No. 05-0626), while the remaining peaks (220, 311, 400, 511, 440 and 331) originate from of the CMFO phase with cubic symmetry and space group $Fd3m$ (JCPDS No. 22-1086). It is very clear that although the main diffraction peaks could be marked as CMFO and BST, some impurity peaks can be observed near 33° and 47°. Further analysis shows that the secondary phase is indexed as $BaFe_{12}O_{19}$, indicating minor chemical reaction between CMFO and BST phases in the composite samples. In addition, the relative height of BST diffraction peaks increases with the molar ratio while the peak intensity of CMFO reduces, signifying the variation of the relative content of the two phases.

To comparatively investigate the surface morphology of the prepared CMFO/BST composite ceramics with different molar ratios, their SEM images were analysed, as shown in Fig. 2. It can be seen that all samples show relative dense surface structure and the gains are most

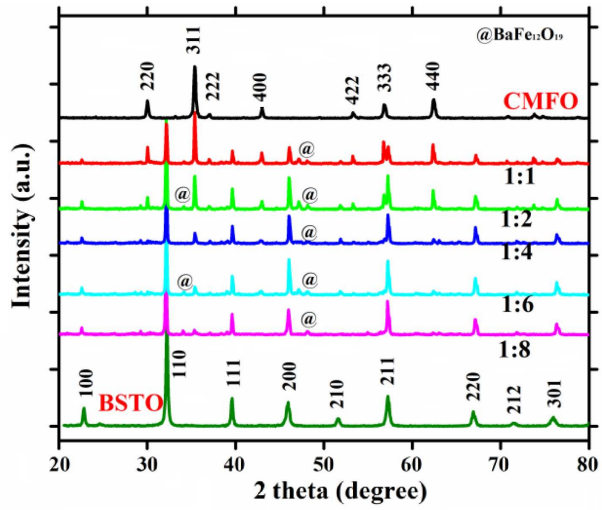

Figure 1. XRD patterns of CMFO/BST composite ceramics with different molar ratios

sphere-like, while the grain size is non-uniform. The average grain sizes calculated by the software Nano Measurer are 1.27, 1.16, 1.03, 1.01 and 1.17 μm (for the molar ratios 1:1, 1:2, 1:4, 1:6 and 1:8, respectively), which decreases first and then increases with the increase of molar ratio. Generally, the appropriate sintering temperature of CMFO is lower than that of BST, therefore, the sintering temperature (1150 °C) for these composites may be higher than that of appropriate sintering temperature of CMFO. The consequence is over-burning of CMFO phase. Hence, when the concentration of CMFO is high, over-burnt ceramics was generated, Fig. 2a, and thus for CMFO grains are the biggest due to too high sintering temperature. With the increase of BST content, the degree of over-burning was restrained, thus smaller grains are obtained. Furthermore, because the sintering temperature of BST is higher than that of CMFO, the addition of BST into CMFO can enhance the optimal sintering temperature of CMFO. Therefore the desired sintering temperature was increased with increasing the concentration of BST, thus the grain size decreases with the molar ratio. When the molar ratio is very high (1:8), the effect of CMFO on the sintering temperature of BST is too weak, thus bigger grain size can be found. Another important factor is that the grain size of BST ceramics is usually very large [19,22], higher content of BST will result in bigger grain size.

In addition, the density also decreases and then increases with the molar ratio, indicating the regulating effect of molar ratio on the shape, density and grain size of the magneto-composite ceramics. Particularly, the density is relatively poor when the molar ratios are 1:4 and 1:6. To directly show the density of the prepared ceramics with different molar ratios, Archimedes principle was applied. When the molar ratios are 1:1, 1:2, 1:4, 1:6 and 1:8, the corresponding densities of the samples are 5.271, 5.267, 5.325, 5.371 and 5.450 g/cm^3, respectively. The relative density was calculated using the ratio of the measured density to the theoretical density.

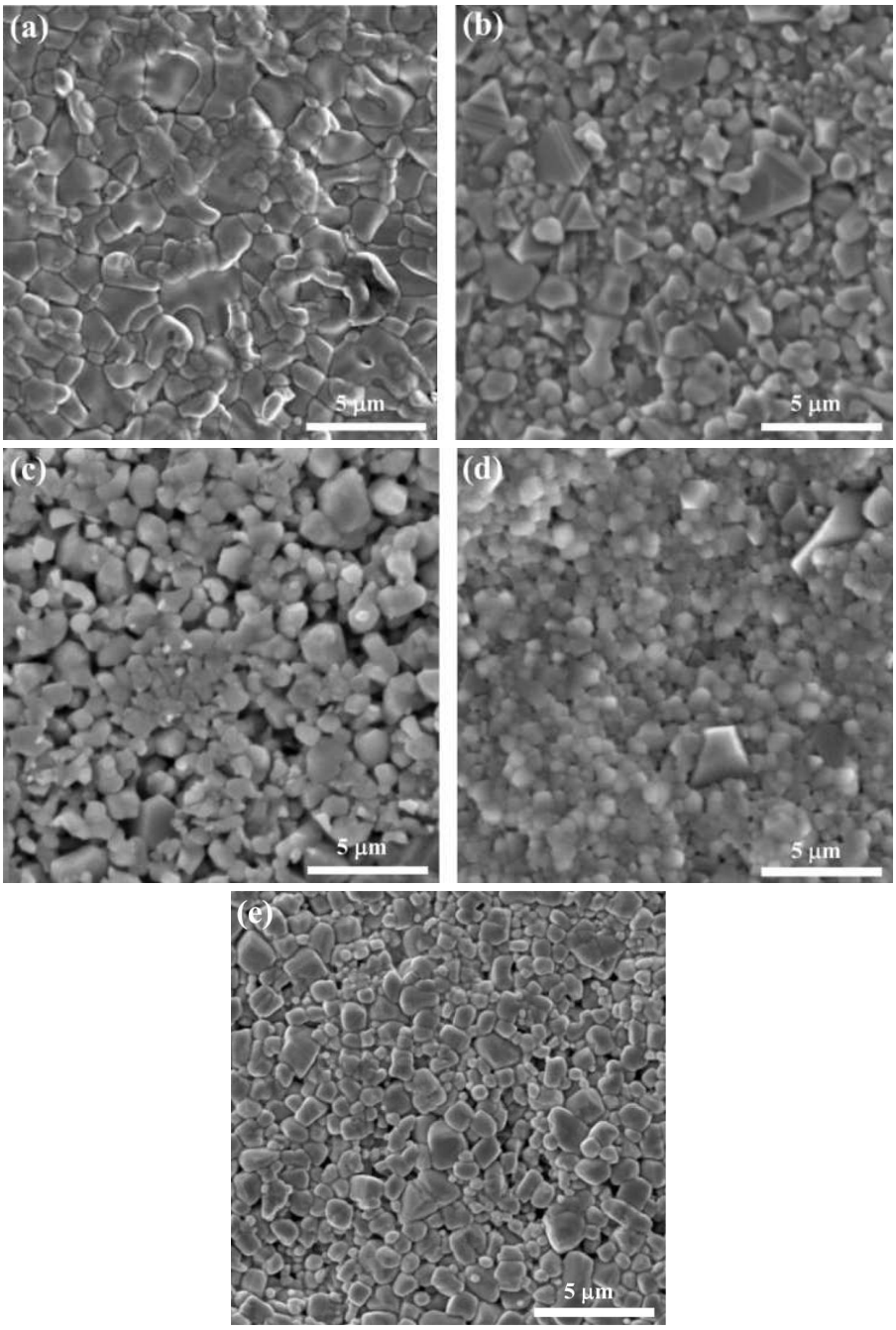

Figure 2. SEM images of the CMFO/BST composite ceramics with different molar ratios: a) 1:1, b) 1:2, c) 1:4, d) 1:6 and e) 1:8

This slight enhancement of the density can be ascribed to the increased compactness resulting from the large grain size and less pores in the samples. The relative densities of the CMFO/BST composite ceramics were 91.8%, 93.7%, 91.4%, 93.2% and 92.3%, and the corresponding porosities were 8.2%, 6.3%, 8.6%, 6.8% and 7.7%, when the molar ratios are 1:1, 1:2, 1:4, 1:6 and 1:8, respectively.

Furthermore, many pores can be observed. This may be the consequence of different optimal sintering parameters between two phases. The pores could be formed during the fast volatilization and violent combustion of PVA adhesives at high temperature, or due to insufficient adhesion of these adhesives. In addition to the influence of PVA, the preforming duration, preforming pressure and powder particle size played significant roles in the formation of pores. Lastly, the grain boundary between the two phases in the composites increased with the decrease of particle size, because only slight chemical reaction occurred between the magnetic and ferroelectric phases. Moreover, the grain growth was inhibited in the ME structure, and thus more pores could be induced, which, in turn, affect the properties of the samples.

3.2. Dielectric properties

The frequency dependent relative dielectric constant (ε_r) and dielectric loss ($\tan\delta$) of the CMFO/BST com-

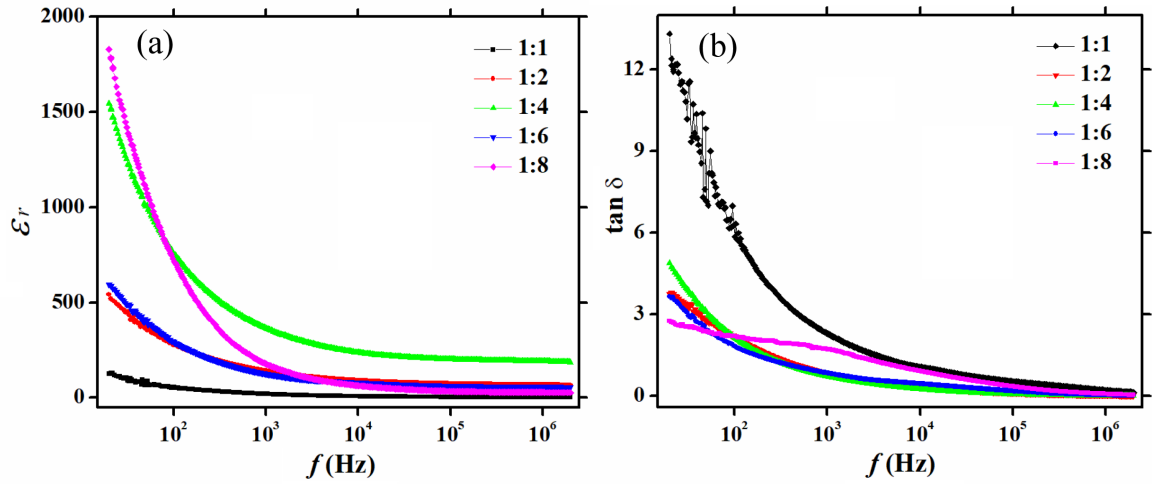

Figure 3. Frequency dependence of the dielectric constant (a) and dielectric loss (b) for the CMFO/BST composites with different molar ratios

posite ceramics are presented in Fig. 3. With the frequency increase, the dielectric constants of all the prepared composite ceramics decrease at first and then they become saturated in the high frequency range, as shown in Fig. 3a. These results can be attributed to various polarization mechanisms at different frequencies. In general, the polarization mechanisms in dielectric materials include displacement polarization and relaxation polarization [25]. The polarization time of displacement polarization, including electronic and ionic displacement polarization, is very short, roughly in the order of 10^{-13} s. In contrast, the polarization time of relaxation polarization, including dipole turning direction, interface, space charge thermal ion relaxation polarization, is relatively longer, which ranges from microsecond to several seconds. When the frequency is low, for example, $f < 1$ kHz ($t > 10^{-3}$ s), almost all the polarization processes can be generated because the polarization times of all polarization mechanism may be smaller than the period of field change. Thus, all polarization mechanisms contribute to the dielectric constant and larger dielectric constant is produced. In contrast, with the increase of frequency, relaxation polarization cannot be evidenced. When the frequency is high (~10^5 Hz), only the displacement polarization can keep pace with the frequency. In that case, the dielectric constant is mainly contributed by the displacement polarization and thus smaller dielectric constant can be obtained.

Nevertheless, it can be seen that the dielectric constant decreases rapidly when the molar ratio is 1:4 and 1:8, while that of other samples declines slowly in the low frequency range. This indicates that the specimens with molar ratios of 1:1, 1:2 and 1:6 show better frequency stability. In the higher frequency range, the dielectric constant of the sample with the molar ratio 1:4 is the maximal while the value is the smallest when the molar ratio is 1:1, as depicted i Fig. 3a. This different variation of dielectric constant with frequency is attributed to the polarization mechanism. The different rate of decrease with frequency indicates that relaxation polarization may be the main polarization mechanism when the molar ratio is 1:4 and 1:8, demonstrating that in these samples more interface charges, dipoles, thermal ions and space charges may exist. These charges may come from the grain boundaries, impurities and pores. More grain boundaries, impurities and pores would induce more charges. Although the grain size and shape can result in different grain boundaries, these differences in all the prepared samples are not that distinct according to the SEM images shown in Fig. 2. Thus, other factors such as oxygen vacancies may be the reason inducing the relaxation polarization.

It is noted from Fig. 3b that the dielectric loss decreases monotonically with increasing frequency, while the decreased trend becomes relatively slow in the high frequency range. The differences between losses in the low frequency range are very obvious while they are unnoticeable when the frequency is high. The sample with the molar ratio of 1:1 shows the highest loss in the low frequency range compared with other samples. This frequency dependent loss is also connected with loss mechanism. The dielectric loss in general includes three parts: the relaxation loss, conduction loss and resonance loss. The relaxation loss is induced by the relaxation polarization, when the polarization process cannot catch up with the speed of external field, loss will be generated. Therefore, the relaxation loss can often happen in the high frequency range. The conduction loss is the result of the conductivity of sample because all samples are not ideal insulators. Obviously, impurities, point defects such as oxygen vacancies, other line and planar defects generated at the grain boundary or phase boundary can give rise to conductance. The third loss is the resonance loss which occurs when the frequency is very high (~10^{13} Hz or more), the vibration of electrons, atoms and molecules will generate heat and result in resonance absorption. With regard to the results shown in Fig. 3b, we can attribute the large loss of the sample (1:1) to the conduction loss because the volume fraction of the magnetic phase is the largest while the conductiv-

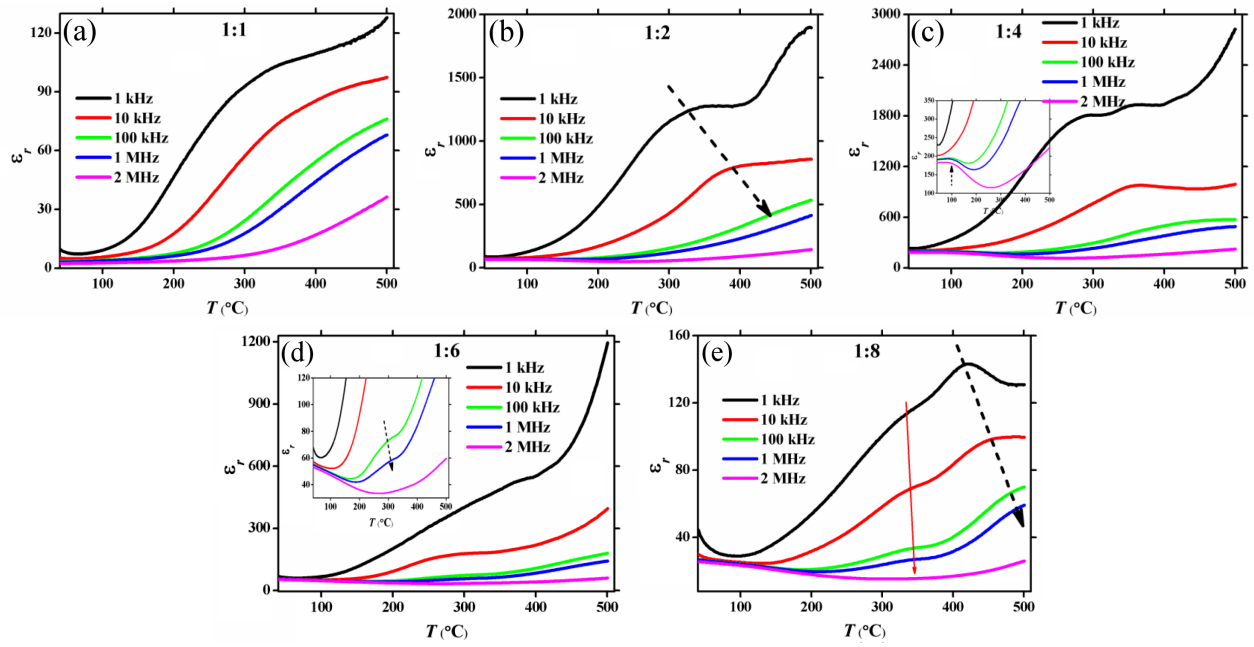

Figure 4. Temperature dependence of the dielectric constant of the CMFO/BST composite ceramics with different molar ratios

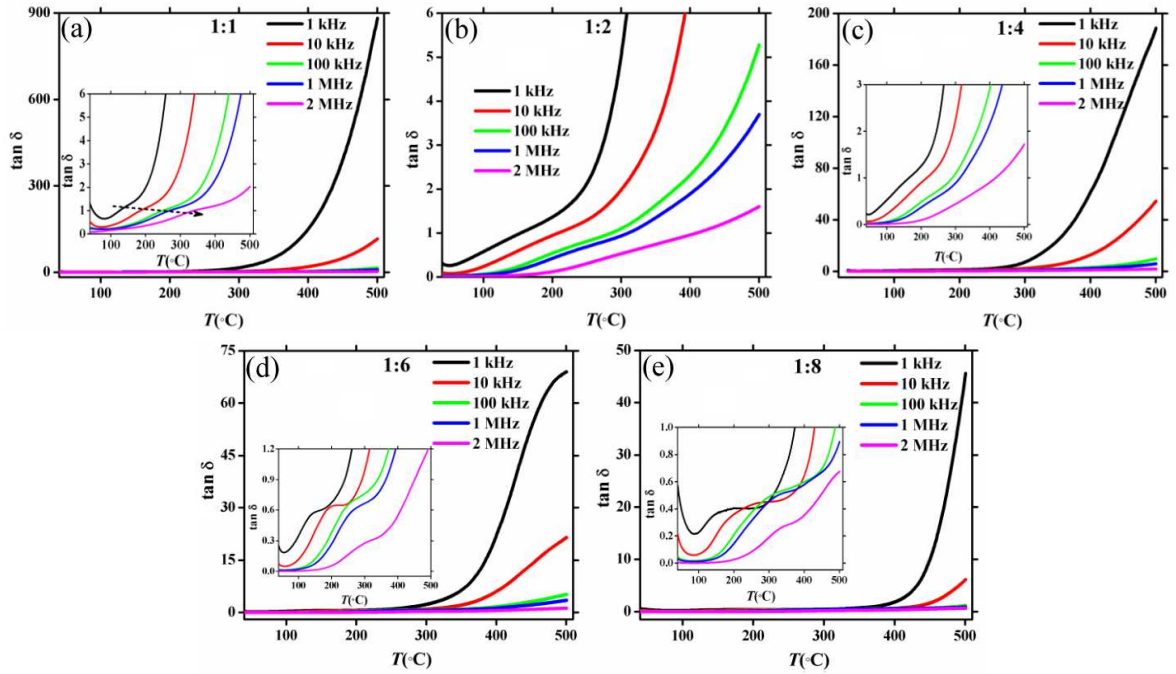

Figure 5. Temperature dependence of the dielectric loss of the CMFO/BST composite ceramics with different molar ratios

ity of CMFO is far higher than that of BST. In addition, when the molar ratio is 1:1, more phase boundaries can be produced and thus more defects can be caused, which in turn gives rise to larger conductivity and dielectric loss.

Figures 4 and 5 describe the temperature (from room temperature to 500 °C) dependence of the dielectric constant and dielectric loss of the CMFO/BST composite ceramics measured at selected frequencies (1 kHz, 10 kHz, 100 kHz, 1 MHz and 2 MHz). It can be seen that the dielectric constant shows non-monotonic variation with the temperature. When the molar ratio is 1:1, a peak can be observed near 300 °C, as shown in Fig. 4a. This temperature may be related with the Curie temperature of CMFO. However, with the increase in frequency, the peak position shifts to higher temperature range and becomes more indistinct while the peak strength declines. Another possible reason for the peak shifting could be the slow polarization due to the frequency and temperature dependence. When the temperature is higher than the corresponding value of the peak, the dielectric constant increases again. This increased dielectric constant may be the result of electron increase in conduction band because more and more electrons

can jump from the valence band to the conduction band with the temperature rise. Correspondingly, a loss peak can also be found near 150 °C at 1 kHz, and this temperature increases to about 350 °C when the frequency is 2 MHz. This loss peak may be ascribed to relaxation loss induced by relaxation polarization. However, in the high temperature range (300–400 °C), no peak can be observed, as shown in Fig. 5a. When the temperature is larger than 300 °C, the dielectric loss rapidly increases with temperature. This significant increase of loss is caused by the increased electronic contribution. More electrons will induce larger conductivity and thus increase of loss can be generated.

Similarly, when the molar ratio is 1:2, a dielectric peak can also be found and it is more distinct, as depicted in Fig. 4b. The peak at the frequency of 1 kHz is near 330 °C, which is slightly lower than that of the sample 1:1, indicating that the concentration of CMFO or BST can tune the relaxation process. The peak value decreases with the increase of frequency, while the peak position shifts with the frequency increasing, as shown by arrow. When the frequency is higher than 10 kHz, no peaks can be observed. This may be because the temperature corresponding to the peak position might be higher than the measuring temperature, i.e. 500 °C. Generally speaking, the dielectric peak is related to relaxation polarization or phase transition process. If it is attributed to the transition temperature of CMFO, the peak should be more apparent with increasing the content of CMFO phase in the composites. However, it can be seen that the peak becomes more distinct with increase of molar ratio, i.e. with decrease of CMFO concentration. Therefore, the dielectric peak can be ascribed to the relaxation polarization. In addition, the dielectric constant for the sample with 1:2 molar ratio increases 10 times compared to the specimen with the molar ratio 1:1. For example, the dielectric constant of the sample with the molar ratio 1:1 is about 90 at 300 °C (f = 1 kHz), while for the molar ratio 1:2, it increases to more than 1200 at the same conditions. As it has been mentioned above, this large dielectric constant can be attributed to the space charges. Another factor that contributes to the larger dielectric constant is the ferroelectric phase BST, which shows high dielectric constant. Although the dielectric constant has been increased more than 10 times, the dielectric loss is obviously smaller than that of the sample 1:1, as presented in Fig. 5b. This smaller loss is the result of the decreased number of electrons in the conduction band because these electrons mainly come from the CMFO component due to its smaller band gap compared with that of BST. With the increase of molar ratio, i.e. the content of CMFO decreases, smaller number of electrons in the conduction band will be induced, thus smaller loss was generated. Although the space charges can induce dielectric loss, the impact is minor compared with the above mentioned effect, especially in the high temperature range.

When the molar ratio is 1:4, both the dielectric constant and loss increase slightly compared with that of the sample 1:2, as shown in Figs. 4c and 5c. When the frequency is 1 kHz, two dielectric peaks can be observed. The first peak is near 300 °C while the higher temperature peak is at about 350 °C. The peak maxima is larger than 1800 at 1 kHz, which is higher than samples 1:1 and 1:2. When the frequency is larger than 1 kHz, the two peaks were transformed into one peak. Though it is not sure what is it made of, it may be related to the relaxation polarization. It can be seen from the SEM images that the pore content is the largest when the molar ratio is 1:4. Therefore, more defects and space charges may be generated and thus relaxation polarization is induced. Slightly increased dielectric constant and loss may be induced by the increased space charges of electrons which were caused by impurities and defects. When the molar ratio is 1:6, both the dielectric constant and loss decrease, and the peak near 300 °C at the frequency 1 kHz disappeared, as presented in Fig. 4d. However, the peak position at the frequency of 10 kHz is below 300 °C. It is found that the peak position decreases with molar ratio on the whole. Interestingly, a loss peak can be observed between 150 to 300 °C when the molar ratio is 1:6, as illustrated in Fig. 5d. The peak position decreases with increasing the test frequency. The peak value and loss of the sample 1:6 are smaller than for other specimens (1:1, 1:2 and 1:4). The reduced dielectric constant and loss may be ascribed to the decreased space charges as a result of the increased content of BST. When the molar ratio is 1:8, the dielectric constant and loss decrease further, as shown in Figs. 4e and 5e. The reason coincided with that of the sample with molar ratio 1:6. What is different is that two dielectric peaks can be found. The first peak (as indicated by arrow) occurs at about 350 °C and it is not obvious, while the second peak is at more than 400 °C. These peaks are also related to the relaxation polarization process.

3.3. Ferroelectric properties

Room temperature polarization-electric field (*P-E*) curves of the CMFO/BST composite ceramics with different molar ratios were shown in Figs. 6 and 7. Both the residual polarization P_r and the coercive field E_c of all the samples increase with increasing the maximal applied voltage, as shown in Fig. 6, indicating that more domains can be switched with increasing the voltage. The ever-increasing E_c with applied maximal voltage can be attributed to the large intrinsic E_i and the serious leakage current of the sample, which can deform the *P-E* curves. Moreover, P_r and E_c decrease with the increase of the measuring frequency, and the ferroelectric hysteresis loops become more and more slender, which can be observed in Fig. 7. Actually, the decreased P_r with the frequency is only a false appearance which is mostly caused by the leakage current of the sample.

In order to investigate the polarization more precisely, *P-E* curves of all the samples are presented with

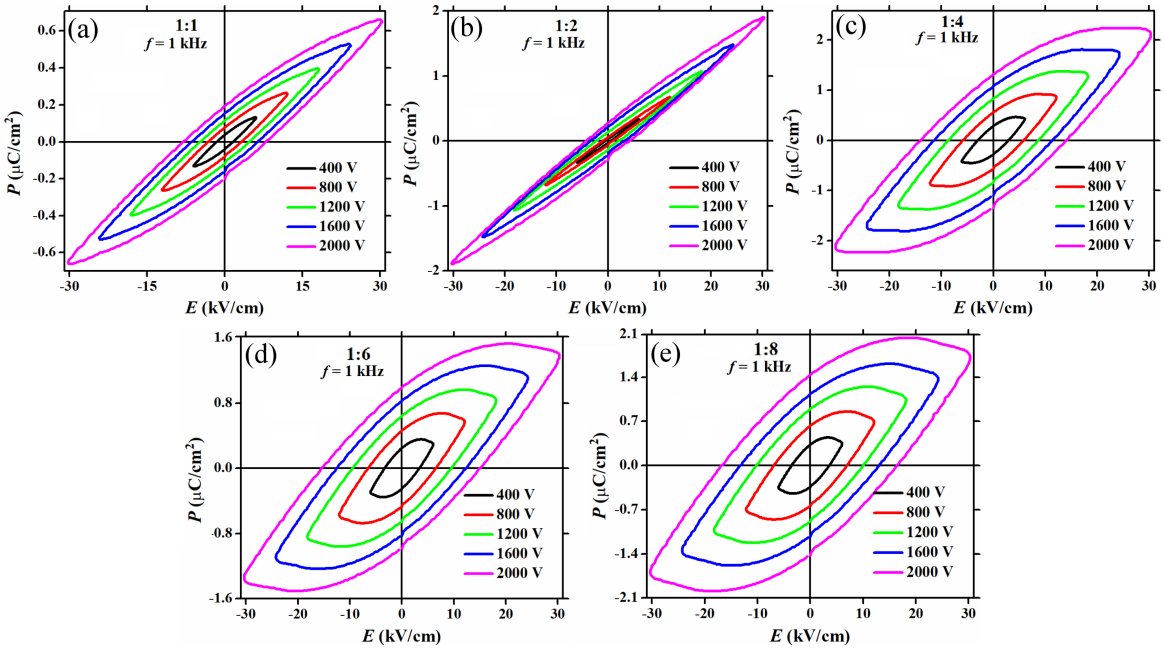

Figure 6. *P-E* curves of the CMFO/BST composite ceramics with different molar ratio measured at different maximal voltages

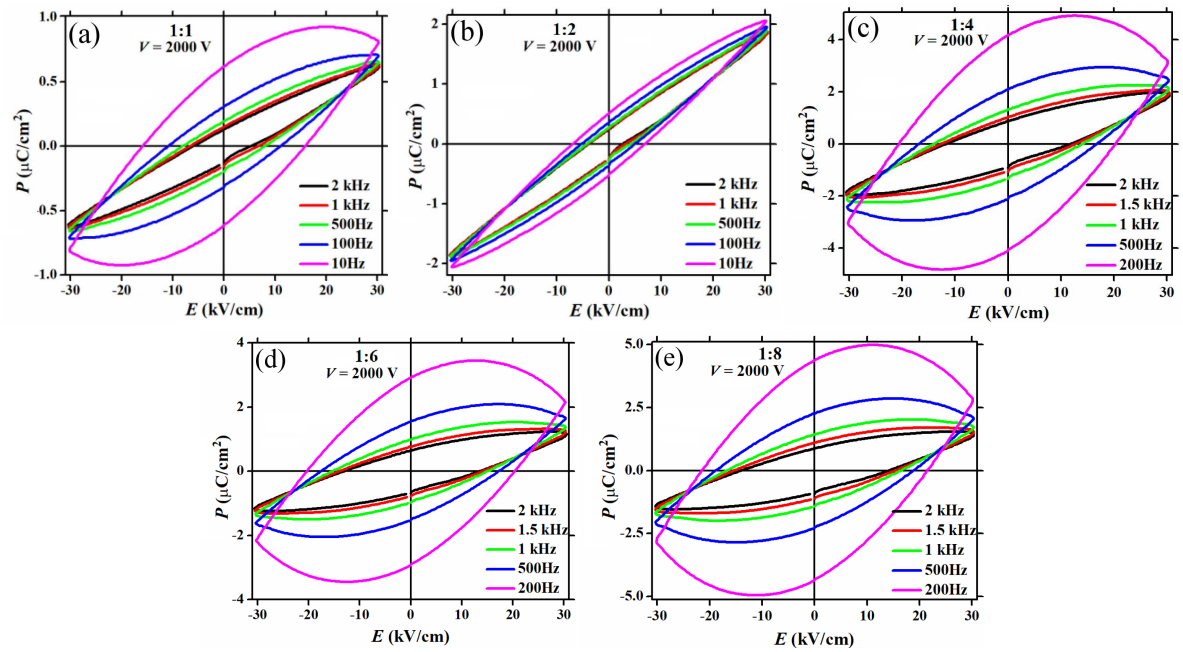

Figure 7. *P-E* curves of the CMFO/BST composite ceramics with different molar ratio measured at different frequencies

the same applied field and frequency, as shown in Fig. 8a. Clearly, P_r increases at first, then decreases and finally it increases again with the molar ratio, while E_c does not show the same variation. The values of P_r are 0.195, 0.275, 1.315, 0.995 and 1.446 μC/cm^2 when the molar ratios are 1:1, 1:2, 1:4, 1:6 and 1:8, respectively. Correspondingly, E_c are 8.15, 4.21, 13.9,15.4 and 16.8 kV/cm, respectively. Generally speaking, the ferroelectric properties should increase with the content of BST in the prepared composite ceramics because CMFO is not ferroelectrics and thus the polarization is entirely contributed by the ferroelectric phase. The monotonic variation phenomenon may be induced by the interface interaction between the two phases or by the leakage current which is caused by the impurities, defects and so forth.

To elucidate whether the abnormal polarization can be affected by the leakage current, the current density-electric field (*J-E*) curves of the composite ceramics are measured at room temperature and shown in Fig. 8b. The difference of the current is very distinct. When the molar ratio is 1:1, the current is at the minimum, while the maximal value can be obtained when the molar ratio is 1:2. This non-monotonic variation of the current with the molar ratio may result from the impurities and defects because the resistivity of BST is higher than that

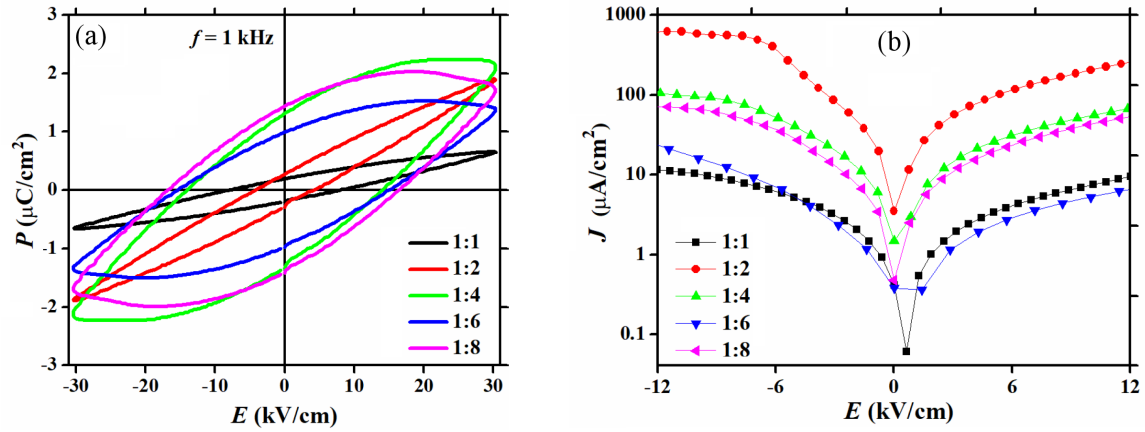

Figure 8. *P-E* (a) and *J-E* (b) curves of the CMFO/BST composite ceramics with different molar ratios

of CMFO. Therefore, with the increase of molar ratio, the current should decrease if there is no interface interaction and chemical reaction between the two phases and without other conditions being changed. As a consequence, we think the sample with the molar ratio of 1:6 seems to show the best ferroelectric properties when Figs. 8a and 8b are combined.

To deduct the contribution of leakage current to the measured polarization, PUND method was applied, as shown in Fig. 9. It can be seen that all curves show perfect rectangular shape, indicating that all specimens have ferroelectric properties. Furthermore, the coercive field of all the samples is nearly the same, but the remnant polarization increases monotonically with the molar ratio. This behaviour is consistent with that predicted theoretically. When the molar ratios are 1:1, 1:2, 1:4, 1:6 and 1:8, the values of remnant polarization are 0.54, 0.70, 0.92, 1.04 and 1.28 μC/cm^2, respectively.

3.4. Magnetic properties

In addition to the dielectric and ferroelectric properties, magnetic properties are also very important for the composite multiferroic materials. In order to evaluate the magnetic properties, room temperature magnetic

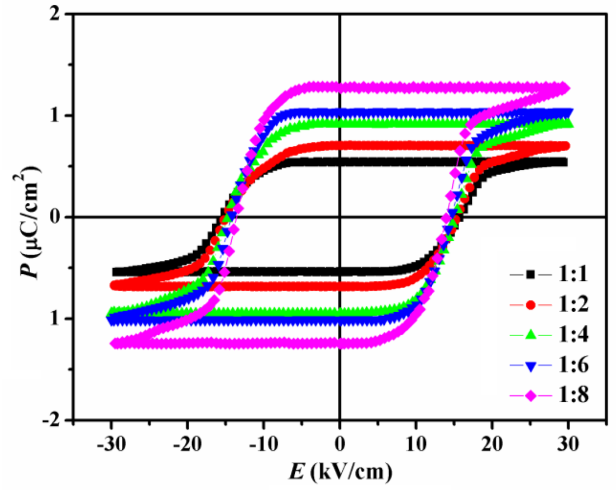

Figure 9. *P-E* curves of CMFO/BST composite ceramics measured by PUND method

hysteresis loops (*M-H* curves) of the CMFO/BST composite ceramics were measured and shown in Fig. 10. A clear hysteresis loops have been observed, indicating the ferromagnetic behaviour. In addition, both the spontaneous magnetization (M_s) and the residual magnetization (M_r) increase first and then decrease with the molar ratio while the coercive field (H_c) show similar phenomenon except minor difference, as listed in Table 1.

Table 1. Magnetic parameters of CMFO/BST composite ceramics

Molar ratio	M_s [emu/g]	M_r [emu/g]	H_c [Oe]
1:1	12.63	6.08	549
1:2	20.89	12.66	830
1:4	7.18	4.14	902
1:6	6.96	4.06	669
1:8	4.53	2.29	291

It is very unusual to find that the highest values for both M_s and M_r can be obtained when the molar ratio is 1:2 and they are 20.89 and 12.66 emu/g, respectively. The minimal values of M_s and M_r are 4.53 and 2.29 emu/g, respectively, when the molar ratio is 1:8. When the molar ratio is 1:4, the maximal H_c can be observed while the minimal value is acquired when the molar ratio is 1:8. Generally speaking, the magnetization of CMFO/BST composite ceramics is mainly contributed by CMFO because BST is non-magnetic and thus the magnetization should be proportional to the molar ratio, i.e. the content of CMFO if there is no interaction between the two phases. Therefore, the largest magnetization of the sample with the molar ratio of 1:2 can be attributed to the larger interface area between the two phases because the interface interaction should enhance with the increase of interface area.

In addition, the intrinsic saturation magnetization of CMFO in different samples may be different because the size and shape of the CMFO grains play an important role in changing the magnetization. As we have presented above that the size and shape of CMFO in the specimens are quite different, therefore, the effective saturation magnetization of CMFO in these samples

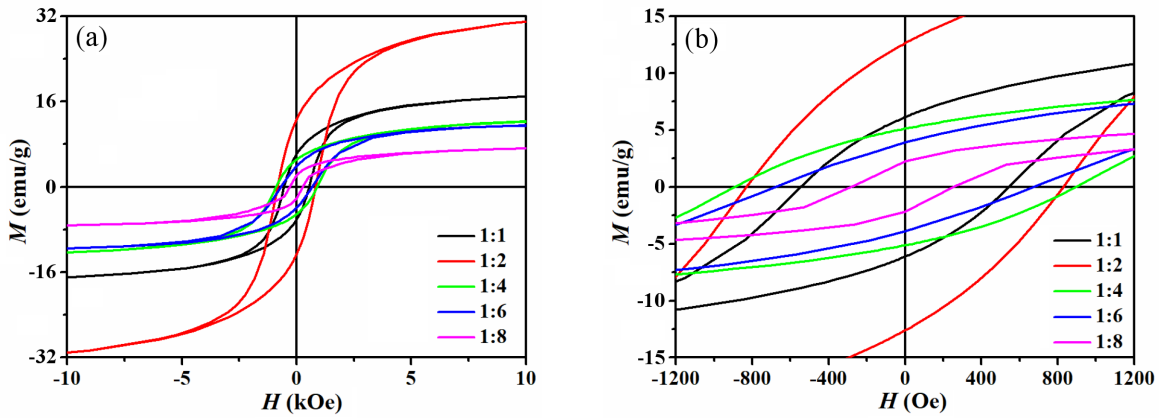

Figure 10. *M-H* curves of CMFO/BST composite ceramics with different molar ratio (a) and the magnified image (b)

should be different. However, in the light of present situation that the effective magnetization of CMFO shows anomalous behaviour, it does not matter if this phenomenon has been induced by the interface interaction or by the grain. It can be considered as a result of the effect of the BST ferroelectric phase on the CMFO magnetic phase in the composite ceramics, which could be considered as a coupling effect.

The highest coercive field of the sample 1:4 may be attributed to the coupling interaction between CMFO and BST, derived from the connective style. Another factor that can affect the coercive field may be the size effect. If the grain size of CMFO is large, the coercive field will increase correspondingly. The contribution of the surface anisotropy constant (K_S) can be described as [27]:

$$K_{eff} = K_{bulk} + \frac{6K_S}{d} \tag{2}$$

where d is the diameter of the particles. Therefore, the surface and its associated anisotropies can play very important role in the case of nanosize particles. However, this difference in grain sizes is not very apparent from the results shown in the SEM images. Actually, the grain size of the sample 1:4 is relatively smaller than other ceramics. In addition, many factors, for example, magnetic anisotropy (including anisotropy such as magnetic crystals, induction, shape and stress), impurities, pores, defects, etc., have major effect on the coercivity. The coercivity determined by boundaries can be expressed as:

$$H_c \approx 3\frac{\gamma_w}{M_s}\frac{1}{D} \tag{3}$$

where γ_w is the domain wall energy, and M_s is the saturation magnetization. γ_w can be expressed as:

$$\gamma_w \approx \sqrt{k \cdot T_c \frac{K_1}{a}} \tag{4}$$

Therefore, H_c can be expressed as follows:

$$H_c \approx 3\frac{\sqrt{k \cdot T_c \frac{K_1}{a}}}{M_s}\frac{1}{D} \tag{5}$$

where k is the Boltzmann constant, K_1 is the magnetocrystalline anisotropy, T_c is the Curie temperature and a is the lattice constant. Briefly, the size effect may be inadequate to account for the magnetic behaviour. It is speculated that the shape of grains or particles, defects, impurities and pores in the sample can also play important roles in the coercive field. The high coercivity value may be enhanced by the anisotropic constant with increasing defects. It can be found from Fig. 2 that the sample 1:4 has the smallest density with the highest number of pores, therefore maximum defects can be formed, increasing the coercive field.

IV. Conclusions

$Co_{0.5}Mg_{0.5}Fe_2O_4/Ba_{0.85}Sr_{0.15}TiO_3$ magnetoelectric bi-phase composite ceramics were successfully prepared by sol-gel method with only slight presence of impurity phases. The mean grain size and the density can be affected by the content of $Ba_{0.85}Sr_{0.15}TiO_3$. The dielectric constant and dielectric loss show non-monotonic variation with molar ratio of CMFO and BST phases and are related to the relaxation polarization and thermally excited electrons. The relaxation behaviour can be tuned by space charges induced by impurities and defects. The sample with the molar ratio 1:8 of CMFO and BST phases shows the highest polarization with the maximal resident polarization of 1.28 °CC/cm. An anomalous magnetic behaviour was observed where the largest saturation magnetization of 20.89 emu/g has the sample with the molar ratio 1:2 due to the stronger interface interaction effect between the two phases. The result may provide valuable information for improving the multiferroic properties of composite multiferroic materials.

Acknowledgement: The present work has been supported by the National Natural Science Foundation of China (Grant No. 11704274), the Chongqing Research Program of Basic Research and Frontier Technology (CSTC2018jcyjAX0416), the Program for Creative Research Groups in University of Chongqing (Grant No. CXQT19031), the Scientific and Techno-

logical Research Young Program of Chongqing Municipal Education Commission (KJQN201801509), the Excellent Talent Project in University of Chongqing (Grant No. 2017-35), the Science and Technology Innovation Project of Social Undertakings and Peoples Livelihood Guarantee of Chongqing (Grant No. cstc2017shmsA90015), the Program for Innovation Teams in University of Chongqing, China (Grant No. CXTDX201601032), the Leading Talents of Scientific and Technological Innovation in Chongqing (CSTC-CXLJRC201919), the Program for Technical and Scientific Innovation Led by Academician of Chongqing, the Latter Foundation Project of Chongqing University of Science & Technology (CKHQZZ2008002), the Scientific & Technological Achievements Foundation Project of Chongqing University of Science & Technology (CKKJCG2016328), the Postgraduate technology innovation project of Chongqing University of Science & Technology (YKJCX1720205) and the student innovating projects of science of Chongqing (YKJCX1820205).

References

1. R.L. Gao, Q.M. Zhang, Z.Y. Xu, Z.H. Wang, W. Cai, G. Chen, X.L. Deng, X.L Cao, X.D. Luo, C.L. Fu, "Strong magnetoelectric coupling effect in $BaTiO_3$@$CoFe_2O_4$ magnetoelectric multiferroic fluids", *Nanoscale*, **10** (2018) 11750–11759.
2. J. Ma, J.M. Hu, Z. Li, C.W. Nan, "Recent progress in multiferroic magnetoelectric composites: From bulk to thin films", *Adv. Mater.*, **23** (2011) 1062.
3. R.L. Gao, Q.M. Zhang, Z.Y. Xu, Z.H. Wang, G. Chen, C.L. Fu, X.L. Deng, W.Cai, "Anomalous magnetoelectric coupling effect of $CoFe_2O_4$-$BaTiO_3$ binary mixed fluids", *ACS Appl. Electron. Mater.*, **1** (2019) 120–1132.
4. S. Dussan, A. Kumar, J.F. Scott, R.S. Katiyar, "Magnetic effects on dielectric and polarization behavior of multiferroic heterostructures", *Appl. Phys. Lett.*, **96** (2010) 072904.
5. R.L. Gao, C.L. Fu, W. Cai, G. Chen, X.L. Deng, H.R. Zhang, J.R. Sun, B.G. Shen, "Electric control of the hall effect in Pt/$Bi_{0.9}La_{0.1}FeO_3$ bilayers", *Sci. Reports*, **6** (2016) 20330.
6. K. Raidongia, A. Nag, A. Sundaresan, C.N.R. Rao, "Multiferroic and magnetoelectric properties of core-shell nanocomposites", *Appl. Phys. Lett.*, **97** (2010) 062904.
7. Q. Zhang, C.H. Kim, Y.H. Jang, H.J. Hwang, J.H. Cho, "Multiferroic properties and surface potential behaviors in cobalt-doped $BiFeO_3$ film", *Appl. Phys. Lett.*, **96** (2010) 152901.
8. J. Wei, R. Haumont, R. Jarrier, P. Berhtet, B. Dkhil, "Non-magnetic Fe-site doping of $BiFeO_3$ multiferroic ceramics", *Appl. Phys. Lett.*, **96** (2010) 102509.
9. R.L. Gao, L. Bai, Z.Y. Xu, Q.M. Zhang, Z.H. Wang, W. Cai, G. Chen, X.L. Deng, C.L. Fu, "Electric field-induced magnetization rotation in magnetoelectric multiferroic fluids", *Adv. Electron. Mater.*, **4** (2018) 1800030.
10. J.H. Lee, H.J. Choi, D. Lee, M.G. Kim, C.W. Bark, S. Ryu, M.A. Oak, H.M. Jang, "Variations of ferroelectric off-centering distortion and 3d-4p orbital mixing in La-doped $BiFeO_3$ multiferroics", *Phys. Rev. B*, **82** (2010) 045113.
11. R.C. Xu, Z.H. Wang, R.L. Gao, S.L. Zhang, Q.W. Zhang, Z.D. Li, C.Y. Li, G. Chen, X.L. Deng, W. Cai, C.L. Fu, "Effect of molar ratio on the microstructure, dielectric and multiferroic properties of $Ni_{0.5}Zn_{0.5}Fe_2O_4$-$Pb_{0.8}Zr_{0.2}TiO_3$ nanocomposite", *J. Mater. Sci.: Mater. Electron.*, **29** (2018) 16226–16237.
12. V. Skumryev, V. Laukhin, I. Fina, X. Martí, F. Sánchez, M. Gospodinov, J. Fontcuberta, "Magnetization reversal by electric-field decoupling of magnetic and ferroelectric domain walls in multiferroic-based heterostructures", *Phys. Rev. Lett.*, **106** (2011) 057206.
13. H.W. Jang, D. Ortiz, S.H. Baek, C.M. Folkman, R.R. Das, P. Shafer, Y.B. Chen, C.T. Nelson, X.Q. Pan, R. Ramesh, C.B. Eom, "Domain engineering for enhanced ferroelectric properties of epitaxial (001) BiFeO thin films", *Adv. Mater.*, **21** (2009) 817–823.
14. R.L. Gao, H.W. Yang, J.R. Sun, Y.G. Zhao, B.G. Shen, "Oxygen vacancies induced switchable and nonswitchable photovoltaic effects in Ag/$Bi_{0.9}La_{0.1}FeO_3$/$La_{0.7}Sr_{0.3}MnO_3$ sandwiched capacitors", *Appl. Phys. Lett.*, **104** (2014) 031906.
15. V. Shelke, D. Mazumdar, G. Srinivasan, A. Kumar, S. Jesse, S. Kalinin, A. Baddorf, A. Gupta, "Reduced coercive field in $BiFeO_3$ thin films through domain engineering", *Adv. Mater.*, **23** (2011) 669–672.
16. H.Q. Zhao, X. Peng, L.X. Zhang, J. Chen, W.S. Yan, X.R. Xing, "Large remanent polarization in multiferroic $NdFeO_3$-$PbTiO_3$ thin film", *Appl. Phys. Lett.*, **103** (2013) 082904.
17. L. You, C.L. Lu, P. Yang, G.C Han, T. Wu, U. Luders, W. Prellier, K. Yao, L. Chen, J.L. Wang, "Uniaxial magnetic anisotropy in $La_{0.7}Sr_{0.3}MnO_3$ thin films induced by multiferroic $BiFeO_3$ with striped ferroelectric domains", *Adv. Mater.*, **22** (2010) 4964–4968.
18. R.L. Gao, Y.S. Chen, J.R. Sun, Y.G. Zhao, J.B. Li, B.G. Shen, "Complex transport behavior accompanying domain switching in $La_{0.1}Bi_{0.9}FeO_3$ sandwiched capacitors", *Appl. Phys. Lett.*, **101** (2012) 152901.
19. T. Woldu, B. Raneesh, B. Hazra, S. Srinath, P. Saravanan, M.V.R. Reddy, N. Kalarikkal, "A comparative study on structural, dielectric and multiferroic properties of $CaFe_2O_4$/$BaTiO_3$ core-shell and mixed composites", *J. Alloys Compd.*, **691** (2017) 644–652.
20. L. Wang, K.J. Jin, C. Ge, C. Wang, H.Z. Guo, H.B. Lu, G.Z. Yang, "Electro-photo double modulation on the resistive switching behavior and switchable photoelectric effect in $BiFeO_3$ films", *Appl. Phys. Lett.*, **102** (2013) 252907.
21. L.P. Curecheriu, M.T. Buscaglia, F. Maglia, C. Padurariu, G. Ciobanu, U.A. Tamburini, V. Buscaglia, L. Mitoseriu, "Tailoring the functional properties of PLZT-$BaTiO_3$ composite ceramics by core-shell approach", *J. Appl. Phys.*, **121** (2017) 144101.
22. L.P. Curecheriu, M.T. Buscaglia, V. Buscaglia, L. Mitoseriu, P. Postolache, A. Ianculescu, P. Nanni, "Functional properties of $BaTiO_3$-$Ni_{0.5}Zn_{0.5}Fe_2O_4$ magnetoelectric ceramics prepared from powders with core-shell structure", *J. Appl. Phys.*, **107** (2010) 104106.
23. P.A. Jadhav, M.B. Shelar, B.K. Chaugule, "Magnetoelectric effect in three phase y ($Ni_{0.5}Cu_{0.2}Zn_{0.3}Fe_2O_4$) + $(1-y)$ (50% $BaTiO_3$ + 50% PZT) ME composites", *J. Alloys Compd.*, **479** (2009) 385–389.
24. B. Raneesh, A. Saha, D. Das, N. Kalarikkal, "Structural and magnetic properties of geometrically frustrated multiferroic $ErMnO_3$ nanoparticles", *J. Alloys Compd.*, **551**

(2013) 654–659.
25. A. Chaudhuri, K. Mandal, "Large magnetoelectric properties in $CoFe_2O_4$:$BaTiO_3$ core-shell nanocomposites", *J. Magn. Magn. Mater.*, **377** (2015) 441–445.
26. S.H. Xie, F.Y. Ma, Y.M. Liu, J.Y. Li, "Multiferroic $CoFe_2O_4$-$Pb(Zr_{0.52}Ti_{0.48})O_3$ core-shell nanofibers and their magnetoelectric coupling", *Nanoscale*, **3** (2011) 3152–3158.
27. J.H. Zou, R.L. Gao, C.L. Fu, W. Cai, G. Chen, X.L. Deng, "Influence of Co ion doping on the microstructure, magnetic and dielectric properties of $Ni_{1-x}Co_xFe_2O_4$ ceramics", *Process. Appl. Ceram.*, **12** (2018) 335–341.